Magneto-Surface Experiments on Germanium

JAY N. ZEMEL AND RICHARD L. PETRITZ
United States Naval Ordnance Laboratory, White Oak, Maryland
(Received January 20, 1958)

A study has been made of the ambient-induced changes in the conductivity, Hall coefficient, and magnetoresistance of thin samples of intrinsic germanium. The data have been analyzed by means of a recently evolved theory. The results indicate that light holes play an important role in the transport process in the surface, especially in the dependence of the zero of the Hall coefficient with increasing surface hole density. It is also shown that there is a reduction of the mobility of surface electrons in qualitative agreement with the predictions of Schrieffer. The results, in general, agree with the current view of semiconductor surfaces.

I. INTRODUCTION

IN the introduction to the preceding paper[1] the importance of directly measuring the density and mobility of charges in the space-charge region of a semiconductor surface was discussed. It was then shown that combined conductivity, Hall coefficient and magnetoresistance measurements could be expected to give such information. These measurements, when carried out with a transverse magnetic field as shown in Fig. 1, do not introduce any additional variables such as surface traps. In principle there should be a unique relationship between the conductivity of a sample, its Hall coefficient, and its magnetoresistance. In I these relationships were evolved. It remains to show that magneto-surface phenomena yield the unique relationship predicted by the theory.

II. EXPERIMENT

A. General Considerations

An examination of Eq. (19) in I indicates that the surface contributions to a Hall or magnetoresistance measurement can be maximized in two ways: (1) reducing the thickness so that the space-charge region is appreciable compared to the physical dimensions of the specimen; and (2) reducing the bulk carrier density, one method being the use of near-intrinsic or intrinsic materials. Because of its convenience, simplicity, and sensitivity, configuration "*a*" described in I was used for the experiment and the surface potential was varied by a modified Bardeen-Brattain cycle.

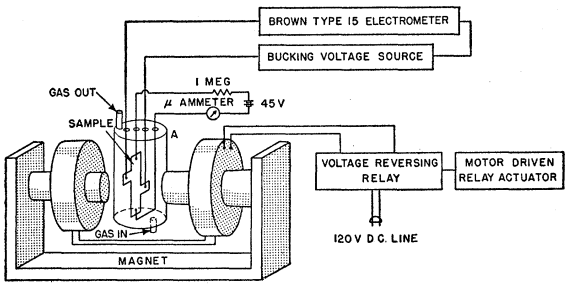

FIG. 1. Experimental arrangement: *A*—gas-tight specimen container; specimen; Brown Type 15 Electrometer; bucking voltage source—Leeds and Northrop Student Potentiometer, 0–1.11 volts.

[1] R. L. Petritz, Phys. Rev. **110**, 1254 (1958), preceding paper (referred to as I).

B. Experimental Arrangement

The schematic arrangement of the apparatus is shown in Fig. 1. A gas-tight brass container, labeled *A*, holds the specimen. The gas was fed into the box as noted from a glass stopcock system. Dry oxygen (breathing purity) was used as the standard ambient. Depending on what was desired, the oxygen could be bubbled through water or passed through a discharge chamber. The discharge was produced by a Tesla coil. By means of these ambients, the surface of the specimen could be driven *n* or *p* type.

The specimen chamber was placed between the pole pieces of a 4-in. electromagnet. The magnetic field, $H(t)$, had a magnitude of 2730 gauss and was cycled with a period of 20 seconds. By means of a motor-driven commutator and mercury relay circuit, the magnetic field was continuously turned on, off, reversed and off in 5-second intervals. The purpose of the alternation of the magnetic field was to permit the simultaneous observation of the sample conductance, Hall voltage, and magnetoresistive signal as the ambient gas affected the surface.

Several specimens were prepared from near-intrinsic (45 ohm-cm) germanium. The samples used had a thickness of 0.004 cm and an impedance in excess of 70 000 ohms. Because of this high impedance, a Brown type 15 vibrating-reed electrometer was used to record potential changes. Because of its degenerative operation, the electrometer measures the open-circuit voltage at the appropriate probes. A low-impedance student-type potentiometer provides a source of bucking voltage used to reduce the IR drop appearing at the electrometer input.

Figure 2 is a typical record of the signal generated at the voltage probes. We can write

$$\begin{aligned} V_1 &= V_{IR}+V_H+V_{\text{mag}} \quad \text{for} \quad H=+|H|, \\ V_2 &= V_{IR}-V_H+V_{\text{mag}} \quad \text{for} \quad H=-|H|, \\ V_3 &= V_{IR} \quad \text{for} \quad H=0. \end{aligned} \tag{1}$$

By simple algebra the Hall voltage, V_H and the mag-

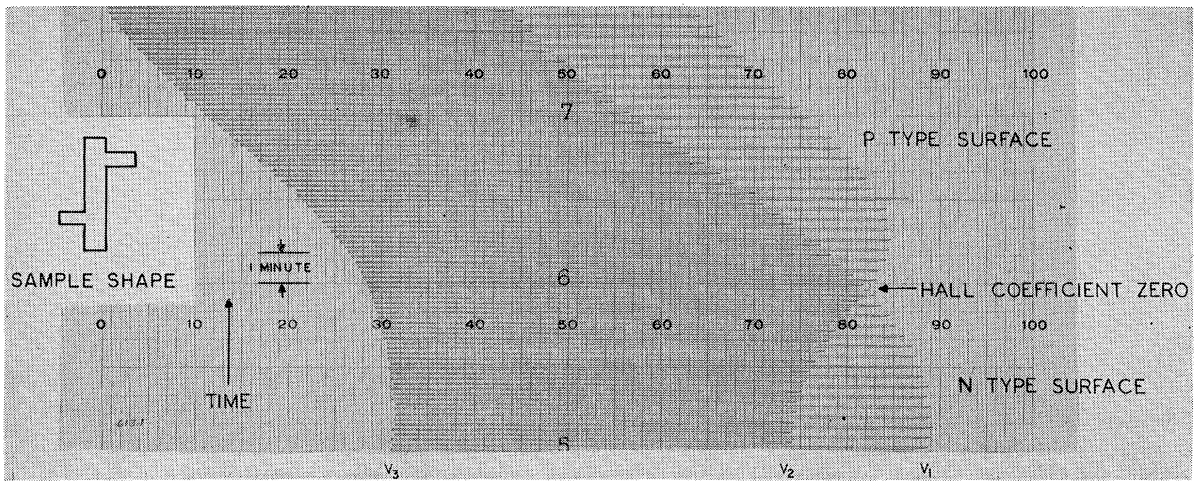

FIG. 2. Typical record of the open-circuit voltage appearing at the probes after the admission of ozone. V_3 is the residual IR drop not taken up by potentiometer circuit. V_1 is the sum of the IR drop, Hall voltage, and magnetoresistive voltage for the magnetic field in a given direction. V_2 is the same sum with the field reversed.

netoresistive change, V_{mag}, can be obtained from this set of equations. The conductance of the sample can be obtained from the IR drop, V_{IR}.

The Hall voltage was found to be approximately linear in current and magnetic field intensity; the magnetic field was kept small (2730 gauss) consistent with obtaining good data. No systematic study was made of the dependence of Hall coefficient and magnetoresistance on field strength.

The sample current was produced by the circuit shown in Fig. 1. A 1-megohm ballast resistor was used to minimize current fluctuations due to changes in the impedance of the specimen. A bank of mercury batteries yielded a driving potential of 45 volts.

C. Sample Preparations

The specimens used were prepared from 0.010-in. thick slices of near-intrinsic germanium. The desired shape was masked and the remaining portions were sandblasted away. The sample was etched to its final thickness by using a 1 part HF and 2 parts HNO_3 solution.

The contacts presented the most difficult problem in the fabrication of the samples. A number of conventional solders and fluxes were tried with no great success. These contacts were ohmic over a very limited range of currents. This problem was solved by using Cerroseal solder[2] and Ruby fluid flux.[3] The contacts prepared in this fashion were substantially ohmic over the range of currents used. After the contacts had been soldered on, the specimen was thoroughly washed in a dilute etching solution to remove all traces of the flux. This was followed by several rinses in distilled water. The specimen was then mounted on a terminal board in such a way that there was a 0.020-in. spacing between the back of the specimen and the terminal board. This was done to permit the ambient to have free access to both sides of the germanium.

[2] Trade name of Cerro de Pasco Corporation, New York, New York.

[3] Trade name of Ruby Chemical Corporation, Columbus, Ohio.

D. Temperature Stability

Because of the large sensitivity of the sample conductance to temperature changes, some degree of temperature stability was needed. This was achieved by placing the specimen container in good thermal contact with the magnet. The magnet was water-cooled from the tap line and the total power input to the magnet was approximately 50 watts. A flow of several liters per minute through the magnet cooling coils assured the maintenance of a magnet and sample temperature within a few degrees of the tap water temperature. The variation of the tap-water temperature was of the order of 0.2–0.3°C over the course of a day. This would lead to an uncertainty of 2–3% in the conductance and Hall voltage. On successive days, the temperature of the water differed by several degrees.

E. Results

In Figs. 3 and 4, the results of several cycles on one of the samples is shown. Figure 3 is a plot of the Hall coefficient,

$$R=(V_H d/IH)\times 10^8 \qquad (2)$$

versus the fractional change in conductivity,

$$\Delta\sigma_{\min}/\sigma_{\min}=(\sigma-\sigma_{\min})/\sigma_{\min}, \qquad (3)$$

where $\sigma_{\min}$ is the minimum conductivity. Figure 4 is a plot of the magnetoresistance coefficient, $\Delta\rho/H^2\rho(H=0)$ *versus* $(\sigma-\sigma_{\min})/\sigma_{\min}$. The data of Figs. 2 and 3 show clearly the reversal of the Hall coefficient of this sample.

We have chosen to use $(\sigma-\sigma_{\min})/\sigma_{\min}$ as the abscissa in these plots for several reasons. First, $\sigma_{\min}$ is a well-

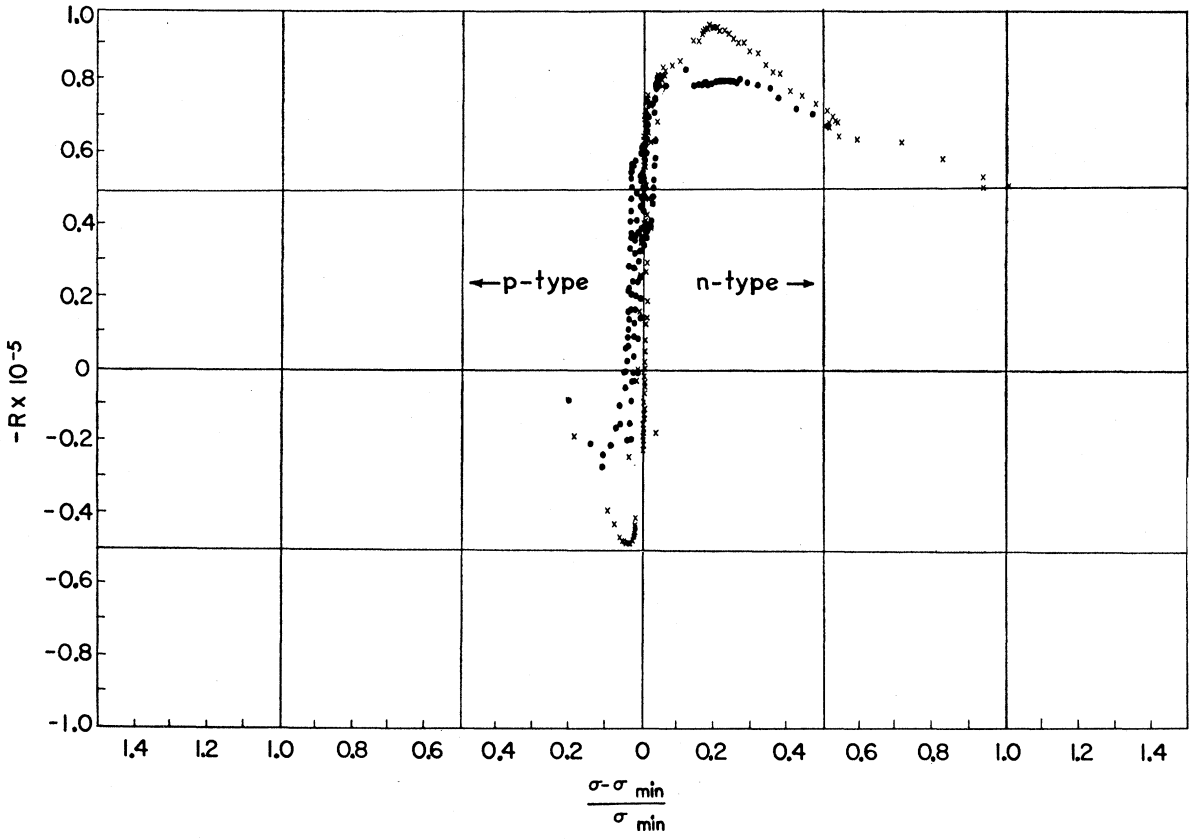

FIG. 3. Hall coefficient as a function of $(\sigma-\sigma_{\min})/\sigma_{\min}$. Increasingly n- and p-type surfaces are indicated by the arrows. Wet oxygen and ozone were used to obtain the n- and p-type surfaces, respectively. These data are a composite of runs made over a period of five days. Small temperature differences could account for the spread in the data.

defined and easily measurable experimental quantity; second, $\sigma_{\min}$ is approximately equal to σ_b (bulk conductivity) in high-resistivity materials, and thus $\sigma-\sigma_{\min}$ is approximately the surface conductivity; and finally, any translation from σ to surface potential involves certain assumptions concerning theory and we prefer not to introduce theory into the presentation of the data. The nature of the surface is indicated on the graphs.

As can be seen, the Hall coefficient is fairly reproducible when plotted as a function of the fractional change in conductivity. Since the Hall coefficient varies quite rapidly near the conductivity minimum, there is greater uncertainty in this region than at the extremes. These data are a composite of runs made over a period of five days. Small temperature differences could account for the spread in the data.

The magnetoresistance data show a very strong dependence on the ambient induced conductivity changes. Of particular interest is the pronounced peak in the data near $\Delta\sigma_{\min}/\sigma_{\min}=0$. The data in Fig. 4 give a broader peak than is the case for an individual run because of the temperature fluctuations from one run to the next.

In general, as time went on, the maximum magnitude of $\Delta\sigma_{\min}/\sigma_{\min}$ decreased. This is attributed to a gradual buildup of the oxide layer and a resultant diminution of the external field due to the adsorbed molecules.

III. THEORETICAL ANALYSIS AND COMPARISON WITH EXPERIMENT

We first describe calculations based on the theoretical work of I.

A. Calculation of the Hall Coefficient and Magnetoresistance Using Bulk Mobilities for Surface Carriers

1. Two-Carrier Model

Our first concern is the general theoretical shape of the Hall coefficient and magnetoresistance as functions of $\Delta\sigma_{\min}/\sigma_{\min}$. We begin with the two-carrier forms of Eqs. (36), (41), and (46) of I, and write down general equations for the conductivity change $\sigma-\sigma_b$, the Hall coefficient R, and the magnetoresistance $\Delta\rho/H^2\rho$. Because of the high-resistivity material we neglect the terms involving n_b and p_b and we also neglect the correlation terms as discussed in I. We then have

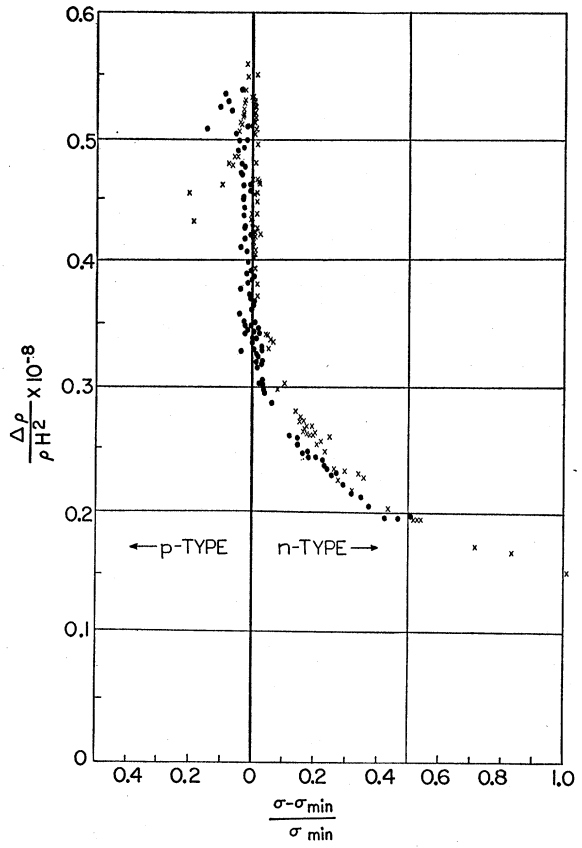

FIG. 4. Magnetoresistive coefficient as a function of $(\sigma-\sigma_{\min})/\sigma_{\min}$. Increasingly n- and p-type surfaces are indicated by the arrows. Wet oxygen and ozone were used to obtain the n- and p-type surfaces, respectively. These data are a composite of runs made over a period of five days. Small temperature differences could account for the spread in the data.

$$\sigma-\sigma_b=(2qL_D/d)(\Delta n_s\langle\mu_{ns}\rangle+\Delta p_s\langle\mu_{ps}\rangle), \tag{4}$$

$$R=-(2qL_D/\sigma^2 d)(\Delta n_s\langle\mu_{ns}^2\rangle - \Delta p_s\langle\mu_{ps}^2\rangle)+R_b(\sigma_b/\sigma)^2, \tag{5}$$

$$\frac{\Delta\rho}{H^2\rho}=\frac{1}{\sigma}\left\{\frac{2qL_D}{d}[\Delta n_s\langle\mu_{ns}^3\rangle+\Delta p_s\langle\mu_{ps}^3\rangle] + \sigma_b\left[\left(\frac{\Delta\rho}{H^2\rho}\right)_b+(R_b\sigma_b)^2\right]\right\}-(R\sigma)^2, \tag{6}$$

where the bulk expressions are

$$\sigma_b=q(n_b\langle\mu_{nb}\rangle+p_b\langle\mu_{pb}\rangle),$$

$$\langle\mu_{nb}\rangle=\mu_n, \quad \langle\mu_{pb}\rangle=\mu_p, \tag{7}$$

$$R_b=-(q/\sigma_b^2)(n_b\langle\mu_{nb}^2\rangle-p_b\langle\mu_{pb}^2\rangle), \tag{8}$$

$$\left(\frac{\Delta\rho}{H^2\rho}\right)_b=\frac{q}{\sigma_b}(n_b\langle\mu_{nb}^3\rangle+p_b\langle\mu_{pb}^3\rangle)-(R_b\sigma_b)^2. \tag{9}$$

The factor 2 has been included because both surfaces were exposed to the ambient gas, i.e., $d\rightarrow d/2$. Using the Poisson model for the space-charge region, we can identify d_s with the Debye length, L_D.

The quantities $\langle\mu^n\rangle$ are the appropriate carrier mobilities for the conductivity, Hall coefficient, and magnetoresistance obtained from the momentum averages discussed in I. In general

$$\langle\mu_{ni}\rangle\neq(\langle\mu_{ni}^2\rangle)^{\frac{1}{2}}\neq(\langle\mu_{ni}^3\rangle)^{\frac{1}{3}},$$
$$\langle\mu_{pi}\rangle\neq(\langle\mu_{pi}^2\rangle)^{\frac{1}{2}}\neq(\langle\mu_{pi}^3\rangle)^{\frac{1}{3}}. \tag{10}$$

The subscript i denotes whether the mobility is associated with the bulk or the surface. We assume lattice scattering in the bulk, so that

$$\langle\mu_{nb}^2\rangle=\tfrac{3}{8}\pi\langle\mu_{nb}\rangle^2, \quad \langle\mu_{pb}^2\rangle=\tfrac{3}{8}\pi\langle\mu_{pb}\rangle^2, \tag{11}$$

$$\langle\mu_{nb}^3\rangle=(4/\pi)(\tfrac{3}{8}\pi)^2\langle\mu_{nb}\rangle^3, \quad \langle\mu_{pb}^3\rangle=(4/\pi)(\tfrac{3}{8}\pi)^2\langle\mu_{pb}\rangle^3. \tag{12}$$

For these first calculations we assume that the surface mobilities can be approximated by their bulk values. Values of Δn_s and Δp_s *versus* the reduced surface potential $\mu_s=q\phi_s/kT$ were taken from the curves of Kingston and Neustadter[4] and are listed for reference in Table I. Using the parameters listed in Table II for intrinsic germanium and Eqs. (4), (5), and (6), a set of curves for $(\sigma-\sigma_b)/\sigma_b$, R/R_b, and $\Delta\rho/[H^2\rho(\frac{3}{8}\pi\mu_n)^2]$ can be calculated as a function of u_s. These curves are shown as solid lines in Fig. 5.

The value of $\sigma_{\min}$ is read from Fig. 5 and using this the quantities can be transformed into functions of $\Delta\sigma_{\min}/\sigma_{\min}$. In Fig. 6 the normalized Hall coefficient,

TABLE I. Surface densities[a] and mobilities[b] used in calculating the theoretical curves.

u_s	$\frac{\Delta p_s}{n_i}=G(u_s,u_b)$	$\frac{\Delta n_s}{n_i}=G(-u_s,-u_b)$	$\frac{\langle\mu_{ns}\rangle}{\langle\mu_{nb}\rangle}$	$\frac{\langle\mu_{ps}\rangle}{\langle\mu_{pb}\rangle}$
−1	1.15	−0.73	1.0	1.0
−2	3.4	−1.25	↓	0.99
−3	6.9	−1.55	↓	0.965
−4	12.5	−1.70	↓	0.935
−5	21	−1.80	↓	0.882
−6	38	−1.88	↓	0.830
−7	67	−1.95	↓	0.755
−8	105	−2.0	↓	0.67
−9	190	−2.0	↓	0.56
−10	310	−2.0	1.0	0.45
+1	−0.73	1.15	0.97	1.0
2	−1.25	3.4	0.945	↓
3	−1.55	6.9	0.90	↓
4	−1.70	12.5	0.845	↓
5	−1.80	21	0.775	↓
6	−1.88	38	0.695	↓
7	−1.95	67	0.595	↓
8	−2.0	105	0.500	↓
9	−2.0	190	0.415	↓
10	−2.0	310	0.323	1.0

[a] Obtained from the curves of reference 2, Figs. 3 and 4.
[b] Obtained from the curves of reference 8, Fig. 4.

[4] R. H. Kingston and S. F. Neustadter, J. Appl. Phys. **26**, 718 (1955).

$R/R_{\max}$, is plotted as the solid curve labeled $b_{32}=0$ against $\Delta\sigma_{\min}/\sigma_{\min}$, where $R_{\max}$ is the maximum value of R in Fig. 5. The magnetoresistance is presented as a function of $\Delta\sigma_{\min}/\sigma_{\min}$ in Fig. 7, with a change in scale factor, $\Delta\rho/[\rho(\frac{3}{8}\pi\mu_n H)^2]\rightarrow\Delta\rho\times10^{-8}/H^2\rho$.

Since we are concerned with the mobility variations of the carriers, a term sensitive to mobility changes is desirable. The quantity $(R\Delta\sigma_{\min}/R_{\max}\sigma_{\min})$ has a greater sensitivity than either the conductivity or the Hall coefficient. This can be obtained directly from Fig. 6. These values are plotted against $\Delta\sigma_{\min}/\sigma_{\min}$ as the solid curve labeled $b_{32}=0$ in Fig. 8.

2. *Comparison with Experiment for Nearly Flat Bands* ($u_s\cong u_b$)

The effects of surface scattering should be negligible for u_s close to zero, so our calculations with $\langle\mu_s\rangle=\langle\mu_b\rangle$ should be adequate to discuss this range. We normalize the data of Figs. 3 and 4 to $R/R_{\max}$, $R\Delta\sigma_{\min}/R_{\max}\sigma_{\min}$ and $\Delta\rho/H^2\rho$, and plot the smoothed data on the corresponding plots of Figs. 6, 7, and 8. These figures then show the normalized data and normalized theoretical curves plotted on the same graph. The general shape of the theoretical curve of $R/R_{\max}$ (solid curve labeled $b_{32}=0$) *versus* $\Delta\sigma_{\min}/\sigma_{\min}$ (Fig. 6) is in rough agreement with the data, with the important exception that the curves does not drop to zero rapidly enough on the p-type side. Consideration of this point leads to the argument that the hole mobility must be increased. It is well known that in bulk germanium there is a small percentage of light, highly mobile holes. Because the mobility is squared in the expression for the Hall-coefficient [Eq. (5)], the light holes have a more pronounced effect on the Hall-coefficient than on the conductivity. We therefore consider the effect of light holes in the calculations to see if better agreement can be found near $u_s=0$.

3. *Three-Carrier Model of Germanium*

The appropriate three-carrier formulas for the conductivity, Hall coefficient, and magnetoresistance are given by Eqs. (36), (41), and (46) of I, respectively. Neglecting the n_b, p_b, and correlation terms, these equations reduce to

$$\frac{\sigma-\sigma_b}{\sigma_b}=\frac{2qL_D}{\sigma_b d}\left[\Delta n_s\langle\mu_{ns}\rangle+\frac{\Delta p_s}{1+r}(\langle\mu_{2s}\rangle+r\langle\mu_{3s}\rangle)\right], \tag{13}$$

$$R=-\frac{1}{\sigma^2}\left\{\frac{2qL_D}{d}\left[\Delta n_s\langle\mu_{ns}^2\rangle-\frac{\Delta p_s}{1+r}(\langle\mu_{2s}^2\rangle+r\langle\mu_{3s}^2\rangle)\right]-R_b\sigma_b^2\right\}, \tag{14}$$

$$\frac{\Delta\rho}{H^2\rho}=\frac{1}{\sigma}\left\{\frac{2qL_D}{d}\left[\Delta n_s\langle\mu_{ns}^3\rangle+\frac{\Delta p_s}{1+r}(\langle\mu_{2s}^3\rangle+r\langle\mu_{3s}^3\rangle)\right]+\sigma_b\left[\left(\frac{\Delta\rho}{H^2\rho}\right)_b+(R_b\sigma_b)^2\right]\right\}-(R\sigma)^2. \tag{15}$$

The bulk expressing are now, assuming lattice scattering,

$$\sigma_b=q\{n_b\langle\mu_{nb}\rangle+[p_b/(1+r)](\langle\mu_{2b}\rangle+r\langle\mu_{3b}\rangle)\}, \tag{16}$$

$$R_b\sigma_b^2=-\tfrac{3}{8}\pi q\{n_b\langle\mu_{nb}\rangle^2-[p_b/(1+r)](\langle\mu_{2b}\rangle^2+r\langle\mu_{3b}\rangle^2)\}, \tag{17}$$

$$\sigma_b\left[\left(\frac{\Delta\rho}{H^2\rho}\right)_b+(R_b\sigma_b)^2\right]=\tfrac{9}{16}\pi q\left[n_b\langle\mu_{nb}\rangle+\frac{p_b}{1+r}(\langle\mu_{2b}\rangle^3+r\langle\mu_{3b}\rangle^3)\right]. \tag{18}$$

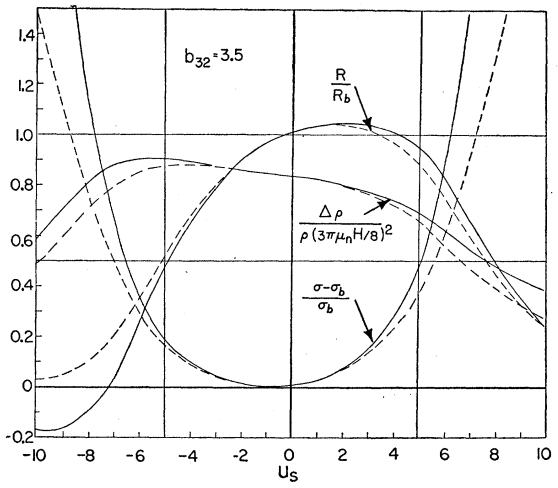

FIG. 5. Two-carrier model of the surface. Conductivity change, Hall coefficient, and magnetoresistance are plotted against the reduced surface potential, u_s. Solid lines correspond to constant surface mobilities, while dashed lines correspond to the mobility variation calculated by Schrieffer for a Poisson potential.

TABLE II. Parameters used in the calculation.

$n_i=2.5\times10^{13}/\text{cm}^3$	No. of intrinsic carriers
$L_D=(\kappa\epsilon_0 kT/2q^2n_i)^{\frac{1}{2}}$ $=6.5\times10^{-5}$ cm	Debye length
$\kappa=16$	dielectric constant
$\langle\mu_{nb}\rangle=\mu_n$ $=3570$ cm²/volt sec	electron mobility in the bulk
$\langle\mu_{pb}\rangle=\mu_p$ $=1745$ cm²/volt sec	hole mobility in the bulk
$b=2.05$	electron-hole mobility ratio in bulk
$d=0.004$ cm	sample thickness
$2L_D/d=3.325\times10^{-2}$	ratio of Debye length to effective sample thickness

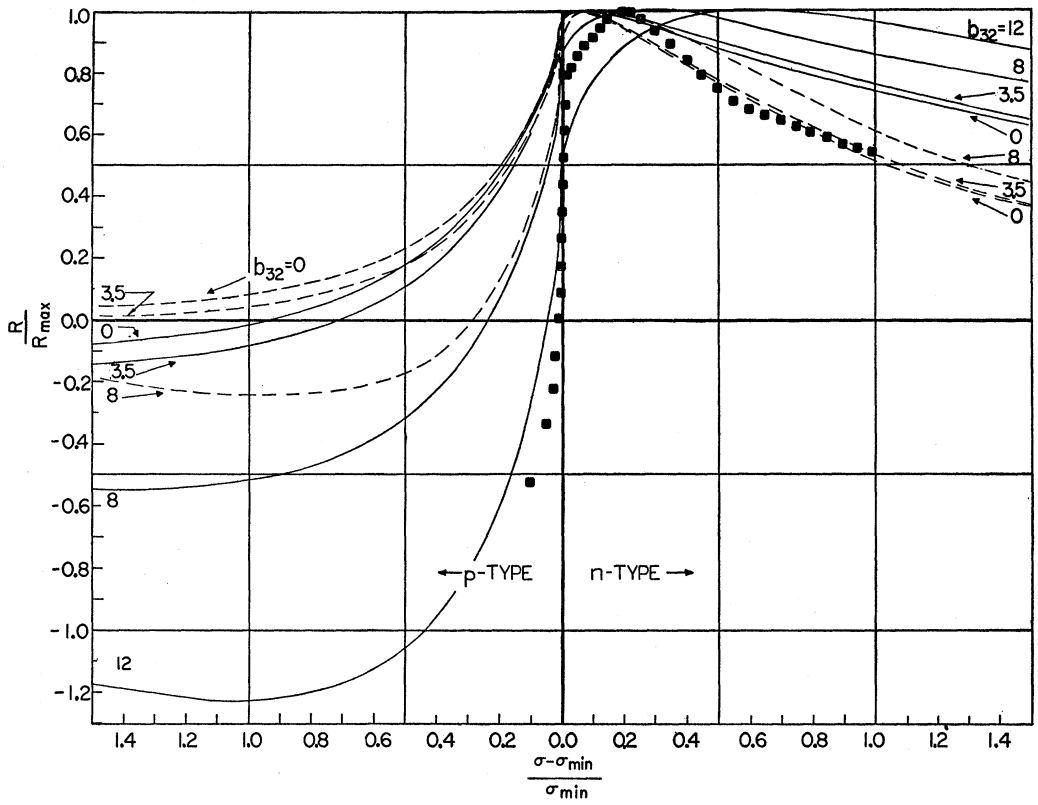

FIG. 6. Comparison of theoretical Hall coefficient with experiment. Two- and three-carrier model Hall coefficients are compared with the smoothed experimental data of Fig. 3, assuming a constant surface mobility (solid lines) and a Schrieffer mobility (dashed lines). The three-carrier model uses light- to heavy-hole mobility ratios of 3.5, 8, and 12 while assuming a density ratio of 0.042.

Two additional parameters enter here,

$b_{32}=\langle\mu_{3b}\rangle/\langle\mu_{2b}\rangle$=ratio of light- to heavy-hole mobility,

$r=n_3/n_2$=ratio of number of light to heavy holes,

where $p_b=n_2+n_3$.

These parameters are known to some degree of accuracy in bulk germanium from cyclotron resonance experiments[5,6] and from Hall-effect and magnetoresistance data.[7–9] However, no given set of parameters appears to fit all the data.[7] Therefore we will consider several possible values in order to study the general effect on our surface quantities.

We have used $r=0.042$ (cyclotron resonance data) in all of our calculations, and have used $b_{32}=3.5$, 8.0, and 12. The value of $\langle\mu_{2b}\rangle$ was set so as to maintain the net hole mobility constant,

$$\langle\mu_{bb}\rangle=(\langle\mu_{2b}\rangle+r\langle\mu_{3b}\rangle)/(1+r)$$
$$=\langle\mu_{2b}\rangle(1+rb_{32})/(1+r)=1745\ \text{cm}^2/\text{volt sec}. \quad (19)$$

Figures 9 and 10 show plots of R/R_b, $(\sigma-\sigma_b)/\sigma_b$, and $\Delta\rho/H^2\rho[(3\pi/8)\mu_n]^2$ *versus* u_s for $b_{32}=3.5$ and 8 respectively (solid curves). These curves are normalized

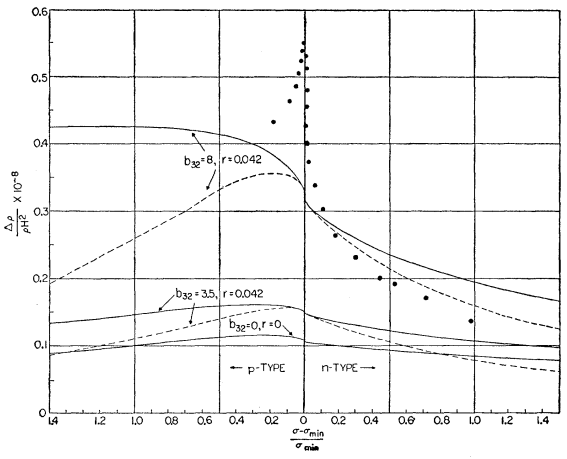

FIG. 7. Comparison of theoretical magnetoresistive coefficient with experiment. Two- and three-carrier model magnetoresistive coefficients are compared with the smoothed experimental data of Fig. 4 assuming a constant surface mobility (solid lines) and a Schrieffer mobility (dashed lines). The three-carrier model uses light- to heavy-hole mobility ratios of 3.5 and 8 while assuming a density ratio of 0.042.

[5] Dresselhaus, Kip, and Kittel, Phys. Rev. **92**, 827 (1953).
[6] Lax, Zeiger, Dexter, and Rosenblum, Phys. Rev. **93**, 1418 (1953).
[7] Goldberg, Adams, and Davis, Phys. Rev. **105**, 865 (1957).
[8] Adams, Davis, and Goldberg, Phys. Rev. **99**, 625 (1955).
[9] Willardson, Harman, and Beer, Phys. Rev. **96**, 1512 (1954).

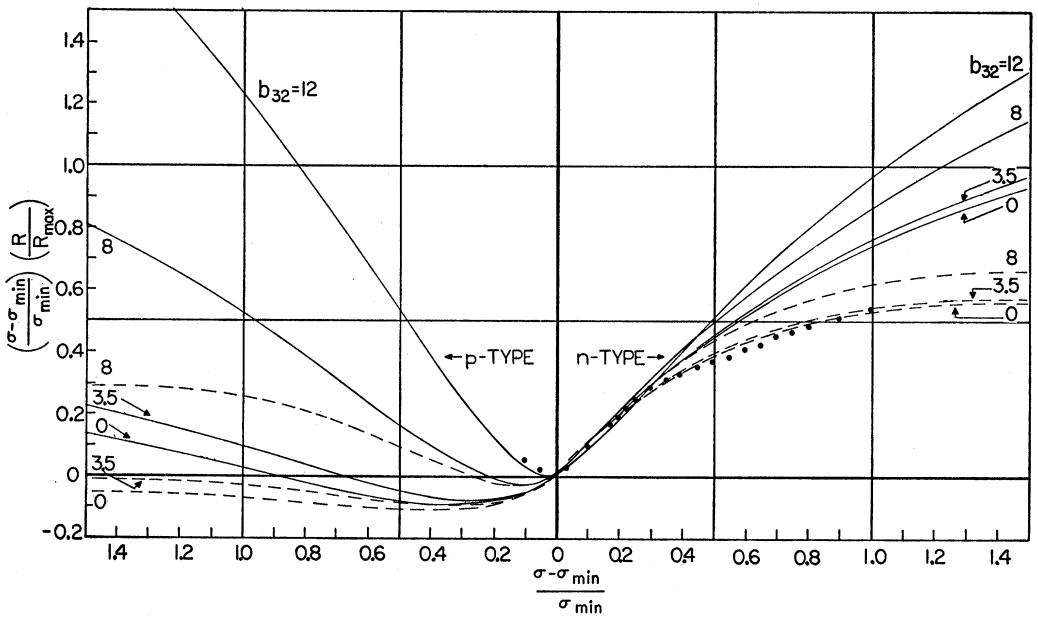

FIG. 8. Comparison of theoretical reduced Hall mobility with experiment. Two- and three-carrier model reduced Hall mobilities are compared with the smoothed experimental data of Fig. 3, assuming a constant surface mobility (solid lines) and a Schrieffer mobility (dashed lines). The three-carrier model uses light- to heavy-hole mobility ratios of 3.5, 8, and 12 while assuming a density ratio of 0.042.

and plotted *versus* $\Delta\sigma_{\min}/\sigma_{\min}$ in Figs. 6, 7, and 8 (solid curves) and labeled by appropriate values of b_{32}. Figure 6 shows that the zero of $R/R_{\max}$ is quite sensitive to light holes. The curves of $b_{32}=8$, 12 agree reasonably well with the data in the region $\Delta\sigma_{\min}/\sigma_{\min}\cong 0$, certainly much better than do the curves of $b_{32}=0$, 3.5. This is evidence that light holes have a pronounced effect on the transport process in the space-charge region.

The magnetoresistance is also quite sensitive to the light holes as shown by Fig. 7, and so is $R\Delta\sigma_{\min}/R_{\max}\sigma_{\min}$ as shown in Fig. 8. We therefore conclude that the light holes must be considered in our analysis.

B. Calculation of Hall Coefficient and Magnetoresistance Using Effective Surface Mobilities

All of the above calculations have been made with the assumption that the mobility in the space-charge region is equal to that in the bulk in order to establish the general theoretical picture, and to discuss the region near $u_s=0$ (flat bands) where surface scattering is negligible. In order to discuss larger swings in surface potential we must include the effects of surface scattering in the theory.

In these calculations we have used Schrieffer's curves[10] of effective surface mobilities *versus* surface potential as tabulated in Table I. For simplicity we have taken $\langle\mu_{2s}\rangle/\langle\mu_{2p}\rangle=\langle\mu_{3s}\rangle/\langle\mu_{3p}\rangle=\langle\mu_{ps}\rangle/\langle\mu_{pb}\rangle$ so that the available curves of Schrieffer for the Poisson model could be used. This assumes that the light- and heavy-hole mobilities are reduced by the same fraction for a given surface potential. This is not strictly correct, as will be discussed further below, but should be adequate for this preliminary discussion.

We also assume that the surface electron mobility is equal to its bulk value when the surface is p type and similarly for the surface hole mobilities when the surface is n type, i.e., specular reflection from the z potential edge. This point is not adequately covered by existing theory, but should not lead to serious error.

A further approximation that has been used is that

$$\langle\mu_{ns}^2\rangle/\langle\mu_{nb}^2\rangle=(\langle\mu_{ns}\rangle/\langle\mu_{nb}\rangle)^2, \tag{20}$$

$$\langle\mu_{ns}^3\rangle/\langle\mu_{nb}^3\rangle=(\langle\mu_{ns}\rangle/\langle\mu_{nb}\rangle)^3, \tag{21}$$

and analogous relations for holes. That is, we assume that the effective "Hall" and "magnetoresistance" mobilities are reduced by surface scattering in the same proportion as the effective "conductivity" mobility. The situation in bulk samples justifies this assumption to some extent; there it is known that such differences are of the order of magnitude of unity. For example, in the case of lattice scattering the relations are given by Eqs. (11) and (12). A second justification of the approximation is the recent solution[11] of $\langle\mu_s^2\rangle$ which shows Eq. (20) to be good to approximately 10%.

The calculation of $(\sigma-\sigma_b)/\sigma_b$, R/R_b, and $\Delta\rho/H^2\rho$ *versus* u_s proceeds as in the previous case, the only difference being that the surface mobilities now vary with surface potential. Calculations have been made for $b_{32}=0$ (two-carrier), 3.5, 8, and 12, keeping $r=0.042$

[10] J. R. Schrieffer, Phys. Rev. **97**, 641 (1955).

[11] J. Zemel, Bull. Am. Phys. Soc. Ser. II, **3**, 105 (1958).

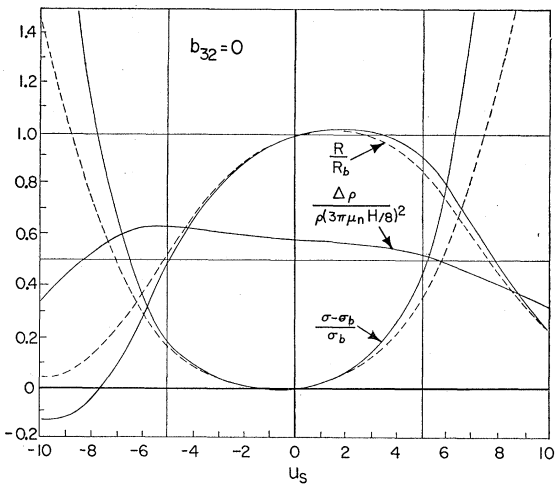

FIG. 9. Three-carrier model of the surface; light- to heavy-hole mobility ratio of 3.5 and density ratio of 0.042. Solid lines correspond to constant surface mobilities while dashed lines correspond to the mobility variation calculated by Schrieffer for a Poisson potential.

except for the two-carrier case, where $r=0$. The results are plotted *versus* u_s as dashed lines in Figs. 5, 9, and 10. Comparison of the dashed with the solid curves shows directly the effects of the reduction in surface mobility.

The curves are transformed to $R/R_{\max}$, $\Delta\rho/H^2\rho$, $R\Delta\sigma_{\min}/R_{\max}\sigma_{\min}$, and plotted *versus* $(\sigma-\sigma_{\min})/\sigma_{\min}$ in Figs. 6, 7, and 8 as dashed lines. Comparison with the appropriate solid lines shows directly the influence of surface scattering. The difference is readily apparent and we conclude from the theory that adequate sensitivity is available to investigate the mechanism of surface scattering.

Throughout the above theoretical anslysis we have considered the samples to be intrinsic. The experimental evidence for this is the resistivity of the samples—about 45 ohm-cm. However this does not determine exactly the bulk Fermi level because the resistivity varies slowly in the region of near-intrinsic material. In contrast, the Hall coefficient and magnetoresistance of the bulk vary quite rapidly in this region. If the sample is close to, but not actually, intrinsic then the theoretical curves cannot be expected to agree completely with experiment. The effect of the uncertainty in the bulk Fermi level will be more serious for the magnetoresistance and less serious for the Hall coefficient.

C. Comparison of Theory and Experiment

Considering first the plot of $R/R_{\max}$ *versus* $(\sigma-\sigma_{\min})/\sigma_{\min}$ (Fig. 6), the sharp drop of the experimental data near $\Delta\sigma_{\min}=0$ indicates a light- to heavy-hole mobility ratio of 8 to 12. On the n-type side the theoretical curve with $b_{32}=8$, and surface mobilities equal to bulk mobilities (solid curve), lies considerably above the data. However, the curve for $b_{32}=8$ and inclusion of surface scattering (dashed curve) more nearly fit the data. The Schrieffer mobility curves for $b_{32}=3.5$ and 0 fit the data very well on the n-type side, but do not drop to zero fast enough on the p-type side.

Consider Fig. 8 where $R\Delta\sigma_{\min}/R_{\max}\sigma_{\min}$ is plotted *versus* $(\sigma-\sigma_{\min})/\sigma_{\min}$. The n-type data are better fitted by using the Schrieffer mobility (dashed curves) rather than the bulk mobility (solid curves) for all values of b_{32}. The best fit is obtained with 0 or 3.5, but that of $b_{32}=8$ is still reasonably good. This plot is regarded as strong evidence for the reduction in surface mobility, and indicates that Schrieffer's theory[10] is in reasonably good quantitative agreement with experiment.

Finally, we consider the magnetoresistance in Fig. 7. The sharp rise in the data on the p-type side is evidence for the presence of light holes since the two carrier theoretical curve does not fit the data at all. The three-carrier, $b_{32}=8$, curves are better, but even they do not rise enough to account for the peak. This suggests a mobility ratio in excess of eight. The Schrieffer mobility correction (dashed curves) improves the fit on both the n- and p-type sides. A further improvement in the theory

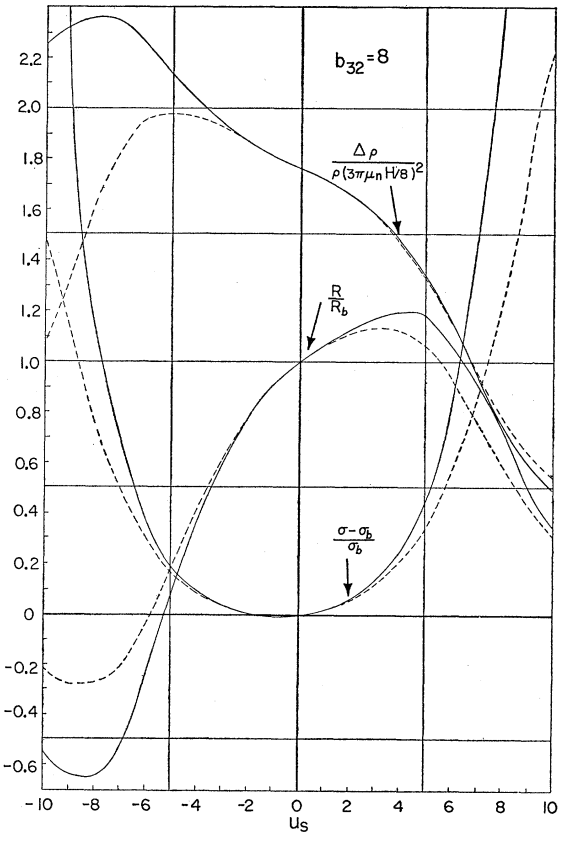

FIG. 10. Three-carrier model of the surface; light- to heavy-hole mobility ratio of 8.0 and density ratio of 0.042. Solid lines correspond to constant surface mobilities while dashed lines correspond to the mobility variation calculated by Schrieffer for a Poisson potential.

will be to treat the light-hole scattering more accurately. As stated before, we have assumed that the mobilities of heavy and light holes are reduced at the same rate. However, one can show that the light-hole mobility should be reduced at a greater rate than that for heavy holes. This correction will result in a more rapid drop of $\Delta\rho/\rho H^2$ on the p-type side. This, combined with a somewhat higher light- to heavy-hole mobility ratio should give a stronger peak in the theoretical curves and agree better with the data.

While the above discussion indicates that there is good qualitative and fair quantitative agreement between experiment and theory for both Hall coefficient and magnetoresistance, there are several points in the experiment as well as the theory which can be refined to give a more exacting test of the surface conduction process. These include: stabilization of the temperature to within the error of the conductivity measurement; determination of the bulk Fermi level by experiment to provide a better starting point for the calculations; a more accurate treatment of bulk and surface carrier mobilities, possibly using a nonspherical energy band model; use of theoretical relations between r and b_{32} rather than varying these quantities independently; and investigation of the dependence of both Hall coefficient and magnetoresistance on magnetic field strength.

IV. CONCLUSIONS AND SUMMARY

We conclude that Hall-coefficient and magnetoresistance measurements can be performed on thin single crystals of germanium to give information concerning the conduction process in the space-charge region of the crystal surface. The experiments reported here are in general agreement with the theory of I and show:

1. The general energy-band structure of germanium describing bulk material also appears to be valid in the space-charge region; there being two types of holes in the space-charge region, with a light- to heavy-hole mobility ratio approximately that found in the bulk ($b_{32}=8-12$), and of about the same density ratio ($r\cong 0.042$).

2. Inclusion of two kinds of holes and one electron allows for qualitative interpretation of the Hall coefficient and conductivity as a function of surface potential, using surface mobilities equal to bulk values.

3. Improved agreement between theory and experiment is attained when Schrieffer's theoretical expressions are used for the surface mobilities. The data are in good qualitative and fair quantitative agreement with the theory, and can be said to be the first direct quantitative evidence of the reduction in surface mobility as a function of surface potential.

4. The magnetoresistance data on the p-type side also confirms the existence of highly mobile holes in the space-charge region. The data support the theory of reduced surface mobility.

These experiments suggest that the present picture of the conduction process in the space-charge region of germanium is a valid one. However, the present studies are limited in that all samples were prepared and treated in essentially the same manner. Of interest is the investigation of the conduction process over a wider range of surface preparations, ambients and temperatures. Materials, other than germanium, should also be investigated. Such a study should determine whether or not the present model has a general validity.

V. ACKNOWLEDGMENTS

The authors would like to express their gratitude to Dr. W. Adcock of the Texas Instrument Company who kindly provided the germanium material used in this work. They would also like to thank Miss Frances Lummis for her help on the calculations.

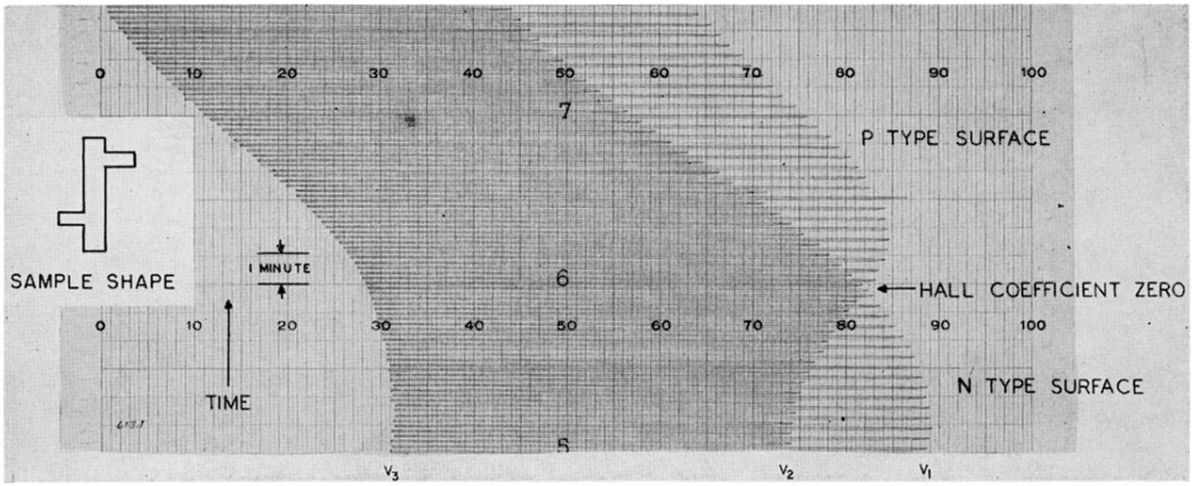

FIG. 2. Typical record of the open-circuit voltage appearing at the probes after the admission of ozone. V_3 is the residual IR drop not taken up by potentiometer circuit. V_1 is the sum of the IR drop, Hall voltage, and magnetoresistive voltage for the magnetic field in a given direction. V_2 is the same sum with the field reversed.